

Laboratory and Computational Fluid Dynamics Investigation of Homogenization in a Tank Stirred by External Pump

Janka Bobek^{1*}, Attila Egedy¹, Dóra Rippel-Pethő¹

¹ Department of Chemical Engineering Science, Faculty of Engineering, University of Pannonia, H-8200 Veszprém, Egyetem str. 10, Hungary

* Corresponding author, e-mail: bobekj@almos.uni-pannon.hu

Received: 15 July 2019, Accepted: 29 October 2019, Published online: 10 December 2019

Abstract

The scope of this study was to investigate the homogenization of a two-layer stratified liquid in a tank where liquid stirring was achieved by carrying out external recirculation. Furthermore, the aim of the research was to observe the effect of the height of the outlet during the time of mixing one. The experimental fluid was two-layer, density stratified liquid. From the perspective of homogeneity, the effect of the height of the outlet was investigated in laboratory. Moreover, the experimental device was modeled in CFD. In simulation examination, laminar - and k- ϵ -model were used, and the influence of the outlet position was observed. The difference was remarkable in the first part of the measurement caused by the presence of sharp concentration variation in the tank. After the operating time, the expected homogeneity was fulfilled at the outlet in all cases. Regarding of CFD research, the results suggest that the laminar model is more effective to describe the concentration changes at the sampling point in the tank investigated.

Keywords

stratified liquid, recirculation, homogenization, laminar model, k- ϵ model

1 Introduction

Homogenization plays a key role in all industrial fields. Inhomogeneity can cause problems in operation and the decadence of product quality can be induced [1]. Usually, good mixing is ensured by stirring or generating turbulence or shear, and it is followed by diffusion at the molecular level [2]. As a result of the mixing, an original non-equilibrium state of a binary mixture is put into the state of equilibrium [3]. One of the most common causes of inhomogeneity can be density stratification. It takes place in case of multi-phase systems or when the liquid to be mixed is immiscible. The stirring of two immiscible fluid such as water-oil system [4] is widely investigated, and gas-liquid stirring [5] is also a well-studied field. The two-phase system has been investigated such as gas-mixed systems [6] including another solution of mixing namely jet stirring [7]. In case of miscible liquids, inhomogeneity can be occurred in several cases, for example when one batch of liquid is loaded on the top of another batch in the same storage tank [8] or when a multi-component liquid needs to be stored for a long time [9]. The contact of two miscible fluids commences mixing processes, which include diffusive mass transfer and initiation of hydrodynamic

flows, but it requires a long time without any external force [3]. Mixing of two-layer stratified liquid in stirred tanks is examined in detail [10]. Usually the mixers operate in turbulent flow regime and only a few studies have worked with laminar flow processes. Laminar flow occurs in case of high viscous liquids and when a recirculation pump stirs the content of the tank with high residence time [11]. Laminar flow can also appear when homogenization is achieved by static mixers [12]. In order to accomplish satisfying mixing, the flow characteristic of the noted system should be obtained. One of the main methods to study mixing in a continuous flow system is the theory of residence time distribution (RTD). The technique is based on the probability distribution of mean age at the exit of the reactor. By analyzing the deviation of the distribution curve of the investigated reactor from the ideal ones, some non-ideal mixing properties can be recognized. RTD method shows the existence of dead zones and bypasses, but the sizes and locations of them cannot be determined [13]. Other methods are yet to be used thorough characterization of dead zones, for example, the Computational Fluid Dynamics (CFD), which is an effective tool to gather

information about mixing. With the help of CFD spatial information can be obtained and the mixing process can be visualized as well, however, choosing of the correct simulation method requires plus efforts [14].

Furthermore, to study the stirring in an industrial scale tank is difficult to carry out by conventional laboratory technics [15], but CFD can be used on an industrial scale, too. In the laboratory, one of the most important tasks is to choose the correct detection system. To discover the changes in the system, the disturbance of the detection system needs to be examined first. Most of the cases the induced probes can disturb the flow field, consequently, we should ascertain that the measuring system does not act as a baffle. In a system wherein the rate of flow is very low, intrusive techniques can be used [16]. Conductometry is an easy way to trace changes in the system and in the end, conductivity values can be converted into concentration data [17]. Conductivity has temperature dependence; for this reason, the temperature compensation is an essential step to retrieve correct values [16].

The aim of this study was to investigate the facilities of intensification of homogeneity in a cylinder tank where the mixing is achieved by an external pump with a low volumetric flow rate. The research is based on an industrial problem where inhomogeneity is occurred due to the density stratification. A batch of the solution is loaded periodically into the tank where the concentration of the main fluid body can differ from the new batch. Owing to the concentration difference and the high residence time, density stratification might occur. The reloaded solution remains in the storage until its usage and before unloading, the content of the tank is mixed by an external pump for a given time. In industry to introduce a change into an existing system is limited by numerous factors in the industry. Authorization of changes in the main construction of a tank or build a baffle or dynamics stirrer in takes a long time. On the other hand, modification in the process has to have the same or higher efficiency and less energy consumption as before at the same time.

For these reasons, the goal of this research was to investigate the effect of the vertical position of the outlet from the perspective of homogeneity in a vessel mixed by an external pump. Measurements were carried out in a laboratory-scale tank with two outlet height (7, 26 mm). To obtain more information about the mixing process where stirring is achieved by external pump, a CFD model of the experimental device was created and the spatial concentration changes were examined. In CFD investigation,

two solution methods were used (laminar and k-ε model) in addition one more outlet height (1 mm) was examined.

2 Materials and methods

2.1 Experimental method

The experimental equipment was a cylinder tank with 194 mm diameter (Fig. 1). The volume of the vessel occupied by the fluid was 3.1 dm³. The model liquid was a two-layer stratified borax solution. The density of stratified liquids was 1002.2 kg m⁻³ and 1013.6 kg m⁻³. This research is based on an industrial problem where the residence time is 3.53 h. For this reason, the constant parameter in laboratory-scale was the residence time, namely 3.53 h. According to the standards, the volumetric flow rate was 0.878 dm³ h⁻¹ = 14.6 cm³ min⁻¹. The inlet (Table 1) was 15 mm above the liquid level. The angle between the inlet and outlet was 110° in all cases. The diameter of the inlet and the outlet was 4 mm. Two outlet positions were examined. Position_0 was 7 mm, Position_1 was 26 mm above the tank bottom (Table 1). Density changes were traced by a two-channel conductivity meter (Consort C3010). Two conductivity probes (Sentek K21, Pt1000) were placed into the system. The conductivity measurements were automatically compensated with temperature. The values of conductivity were sampled in every 30 seconds, and the experimental data were recorded in a PC via Consort DIS-1. One of the probes was always sampling the outlet (CH2); therefore, the vertical position of sampling point CH2 was changed with the vertical position of the outlet. The other sampling point (CH1) was in a fix position during all experiments (Table 1).

At the beginning of all experiments, the content of the tank was a stratified two-layer liquid. 1.55 dm³, 1013.6 kg m⁻³ solution was stratified under the 1.55 dm³,

Table 1 Position of inlet, outlet and sampling points

| | Position_0 | Position_1 |
|--------|-----------------------|--|
| Inlet | | x = 97 mm y = 120 mm z = 0 mm |
| Outlet | y ₀ = 7 mm | x = -17 mm y ₁ = 26 mm z = -45 mm |
| CH1 | | x = 64 mm y = 67 mm z = 64 mm |
| CH2 | y ₀ = 3 mm | x = -17 mm y ₁ = 15 mm z = -30 mm |

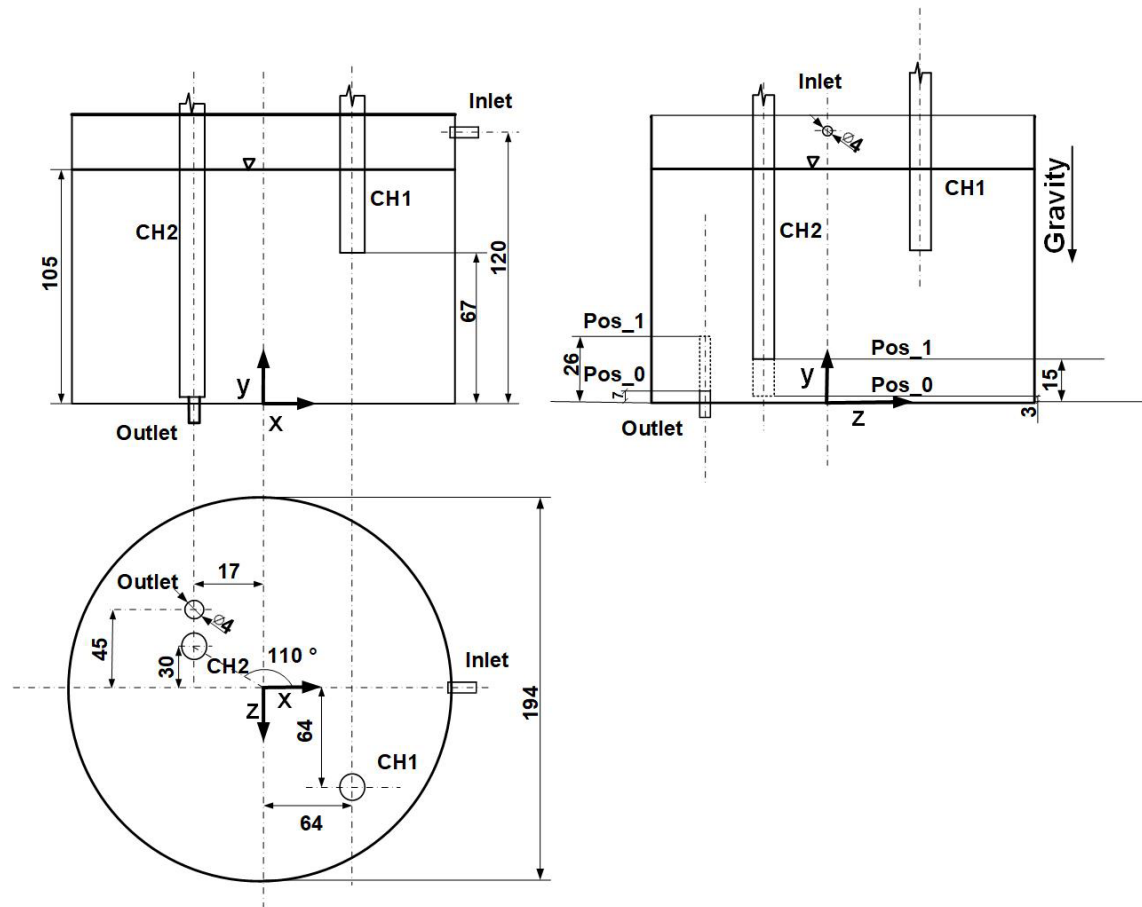


Fig. 1 Schematic of positions of the inlet, the outlet and the sampling points in mm

1002.2 kg m⁻³ liquid (Fig. 2). The outlet of the experimental tank (1.) was pumped into the buffer tank (3.) by a peristaltic pump (2.). The inlet flow rate of the experimental tank was ensured by gravity flow from a buffer tank (3.), and it was checked on a rotameter (4.).

Before the experiments, the position of the buffer tank was set, and the inlet flow rate was checked. The overflow-outlet of the buffer tank (3.) was also built into the system however, the fluid level was constant, therefore no overflow was noticed in the no. 5. storage tank. After all experiments, the tank content was stirred manually to check the final value of density. It was necessary to convince that inhomogeneous fluid elements did not remained in the system. Measurements were carried out over 900 minutes, at ambient temperature.

2.2 Computational method

Ansys Fluent was used to gather information about fluid flow and to approximate the laboratory results. First, the geometry was built with the same construction as in the laboratory; the two-layer system was established in this step (Fig. 3 (a)).

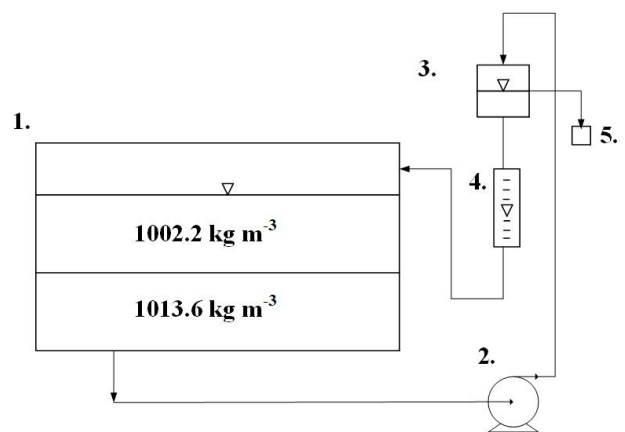


Fig. 2 Schematic of experimental setup

At laboratory measurements, the inlet flowed on the wall. In consequence, the model was built as a one-phase system and the inlet surface was calculated from the average velocity in the equation of laminar flow down an inclined plane surface [18]. The average velocity of the falling film was determined by Eq. (1), where ρ was the density of the liquid, g was the gravitational acceleration,

L was the film thickness, φ was the angle between the plane and the film (90°) and μ was the dynamic viscosity.

$$v_{av} = \frac{\rho g L^2 \sin \varphi}{3\mu} \quad (1)$$

The film thickness (L) was calculated from Eq. (2), where B was the volume rate of flow and W was the cross-section of the film.

$$L = \sqrt[3]{\frac{3\mu B}{\rho g W \sin \varphi}} \quad (2)$$

Velocity components in direction x and z were equalled to 0 m s^{-1} , while in direction y it was equivalent to $-v_{av}$, namely -0.231 m s^{-1} (Eq. (1)). The area of the inlet surface ($1.06 \cdot 10^{-6} \text{ m}^2$) (Fig. 3 (b)) was implemented as a semicircle and it was calculated from the average velocity as well as the volume flow rate. In this study, to investigate the mixing effects in a cylinder tank stirred by an external pump, two different strategies were used, namely the laminar model and the realizable $k-\varepsilon$ model. On first thought, due to the long residence time (3.53 h) and the low inlet flow rate ($0.878 \text{ dm}^3 \text{ h}^{-1}$), the laminar model might be a satisfying solution to simulate the concentration changes in the system. Generally, motions of fluids are governed by the continuity equation (Eq. (3)).

$$\frac{D\rho}{Dt} + \rho \nabla v = 0 \quad (3)$$

To solve liquid-liquid mixing problems, numerical methods based on Navier-Stokes equation (Eq. (4)) should be taken into consideration which is the differential form of Newton's 2nd law.

$$\rho \frac{D\mathbf{v}}{Dt} = \mathbf{F} - \text{grad } p + \text{Div } \tau \quad (4)$$

$$\tau = \mu \left(2\varepsilon - \frac{2}{3} \delta \text{ div } \mathbf{v} \right) \quad (5)$$

The realizable $k-\varepsilon$ model provides excellent performance for flows involving rotation, boundary layers under strong adverse pressure gradients, separation and recirculation [14]. Realizable $k-\varepsilon$ model is one of the most often used turbulence models which is generally based on Reynolds-stresses, $(\rho \overline{u'_i u'_j})$, modified Navier-Stokes equation (Eq. (6)) [18].

$$\rho \frac{D\overline{u}_i}{Dt} = F_i - \frac{\partial \overline{p}}{\partial x_i} + \frac{\partial}{\partial x_j} \tau_{ij} \quad (6)$$

$$\tau_{ij} = \mu \frac{\partial \overline{u}_i}{\partial x_j} - \rho \overline{u'_i u'_j} \quad (7)$$

With the approach of the eddy viscosity principle after Boussinesq, the total shear stress can be written down by kinetic energy (k) and turbulent viscosity (ν_T) (Eq. (8)).

$$\tau_{ij} = \mu \frac{\partial \overline{u}_i}{\partial x_j} + \rho \left(\nu_T \left(\frac{\partial \overline{u}_i}{\partial x_j} + \frac{\partial \overline{u}_j}{\partial x_i} \right) - \frac{2}{3} k \delta_{ij} \right) \quad (8)$$

The transport equation for turbulent kinetic energy (k) and its dissipation rate (ε) are calculated with Eq. (9) and Eq. (10).

$$\frac{\partial}{\partial t} (k\rho) + \frac{\partial}{\partial x_i} (\rho k u_j) = \frac{\partial}{\partial x_j} \left[\left(\mu + \frac{\mu_T}{\sigma_k} \right) \frac{\partial k}{\partial x_j} \right] + P_k - \rho \varepsilon \quad (9)$$

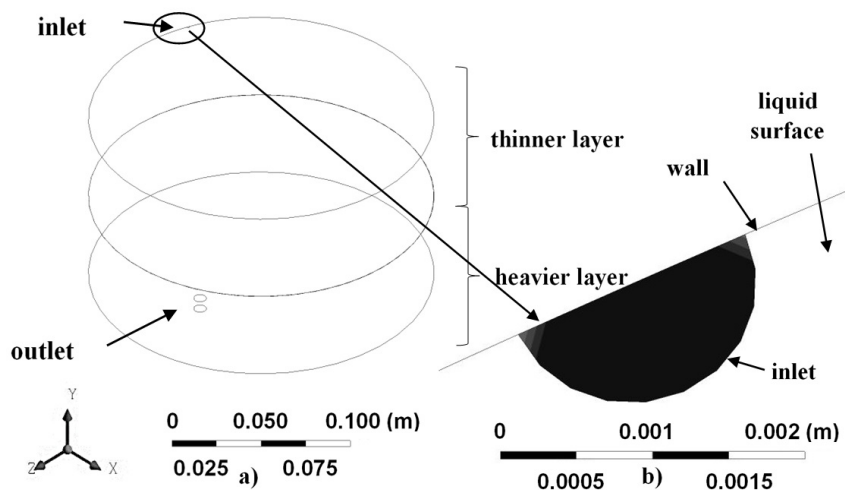


Fig. 3 a) Geometry of the investigated tank b) Magnified picture of the inlet

$$\frac{\partial}{\partial t}(\varepsilon\rho) + \frac{\partial}{\partial x_j}(\rho\varepsilon u_j) = \frac{\partial}{\partial x_j} \left[\left(\mu + \frac{\mu_T}{\sigma_\varepsilon} \right) \frac{\partial \varepsilon}{\partial x_j} \right] - \rho C_2 \frac{\varepsilon^2}{k + \sqrt{\varepsilon\nu}} + C_{1\varepsilon} \frac{\varepsilon}{k} P_k \quad (10)$$

The model constantans in the realizable k- ε model were given by Launder and Spalding: $C_{1\varepsilon} = 1.44$, $C_2 = 1.9$, $\sigma_\varepsilon = 1.2$, $\sigma_k = 1.0$ [19]. The influence of the wall was emphasized by the enhanced wall treatment setup.

In the solution process, coupled scheme was chosen for pressure-velocity coupling and second-order special discretization and transient formulation were set in all cases.

For the calculation, the component transport equation (Eq. (11)) was used. The density was fitted with concentration by a second-degree polynomial equation (Eq. (12)) and considering the density of 0 kg m^{-3} borax solution is equal to 1000 kg m^{-3} .

$$\frac{\partial c}{\partial t} = -\text{div}(\mathbf{vc}) + \text{div}(D \text{ grad}c) \quad (11)$$

$$\rho = A_0c^0 + A_1c^1 + A_2c^2 = 1 + 0.18 \cdot c + 0.004c^2 \quad (12)$$

A user-defined function (UDF) was applied to calculate the recirculation in the model. The calculus of the program is based on the node number of the outlet surface, and the concentration is calculated on the nodes of the same surface. The concentration values on the outlet were averaged with the number of nodes on the surface. The calculated average concentration was the time-delayed inlet value of concentration to achieve similar operation regarding the experiments. In the beginning, the upper layer was identified with 1002.2 kg m^{-3} , and the lower was constant 1013.6 kg m^{-3} . CFD investigation was implemented over 9000 time steps with regard to 1 time step was equal to 1 s consequently, the total mixing time was 150 min.

3 Results and discussion

The object of this study was to achieve a CFD model to investigate the effect of the vertical position of the outlet on homogenization of a two-layer stratified liquid in a cylinder tank.

3.1 Mesh independence study

The mesh independence study (Fig. 4) was carried out on laboratory results of Position_0 with 7 mm outlet height.

The error value was calculated onto the concentration rates between 120-150 minutes compared to the experimental results. The error, in percent, was given by the value of absolute inaccuracy over steady-state values of the

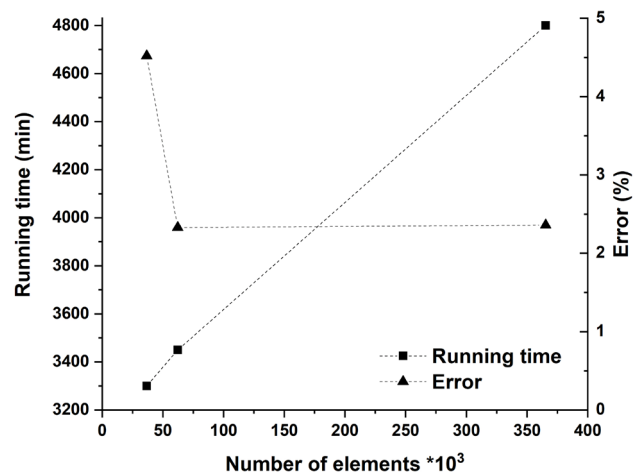


Fig. 4 Mesh independence study

laboratory measurement. The aim was to find a convenient mesh element number, which satisfies the accuracy demand and does not consume too long running time to achieve 9000 time steps. CFD researches were carried out with $\sim 62 \cdot 10^3$ elements number.

3.2 Laboratory and CFD results

In the laboratory, the outlet results were calculated by the concentration values measured at CH2 (Table 1). In CFD simulations, the outlet results were equal to the node number averaged concentration on the outlet surface. Homogeneity (Eq. (13)) was calculated into the outlet stream from the concentration data to achieve better comparability of the results. Homogeneity was calculated with the help of the actual concentration difference ($c_t - c_{av}$) and the total concentration difference (Δc).

$$H_t (\%) = 100 - \left(\frac{|c_t - c_{av}|}{\Delta c} \right) \cdot 100 \quad (13)$$

Analyze the CFD and laboratory results in Fig. 5 the influence of the vertical position of the outlet can be seen. At 7 mm outlet position (Fig. 5 (a)) the homogeneity is improved sharply in the first 35 min and finally it remains nearly constant. The homogeneity results at both CFD models are increased more exponentially than one can see in the laboratory curve. The results of the laminar model are below the k- ε model values until 75 min. After 75 min the position of the curves changed. As time passes by, the results are nearly the same at both models. Laboratory result with 26 mm outlet position (Fig. 5 (b)) has more exponential growth compared to the result at 7 mm. The simulation curves show the same in case of CFD results of 7 mm set. The homogeneity results at the same time at the k- ε model are higher than the

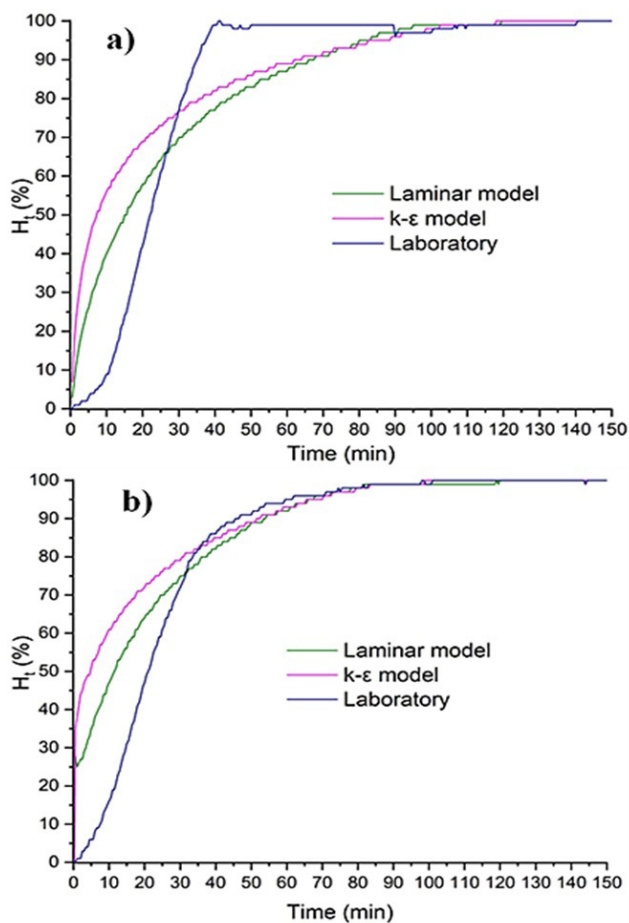


Fig. 5 a) Homogeneity results at 7 mm outlet position b) Homogeneity results at 26 mm outlet position

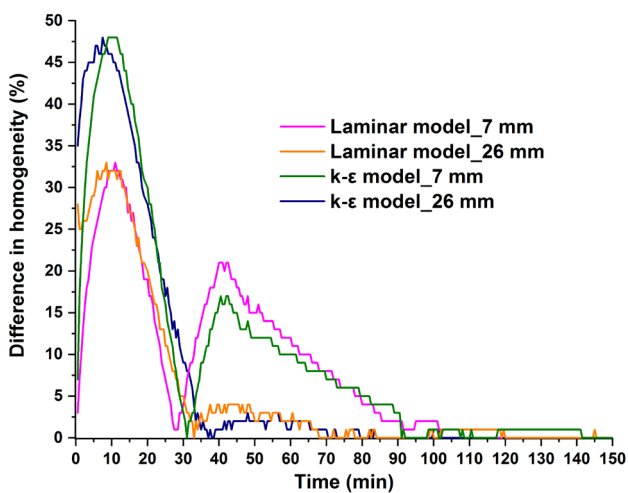


Fig. 6 Difference in CFD homogeneity results compared to laboratory

results of the laminar model. After 50 min, the simulation and laboratory results run together.

After the laboratory measurements had been finished, the tank content was mixed manually. Concentration changes were not recognized at any sampling points (CH1,

CH2). However, the conductivity difference was not recorded after stirring, nevertheless it does not necessarily mean that the entire fluid body is homogenous.

In Fig. 6 comparing values extracted from CFD and laboratory results the diversity in homogeneity can be seen. The calculated homogeneity difference (ΔH_t) was equal to the difference between simulation and laboratory homogeneity at the same time at the outlet. To begin with, the first 30 min measuring time, peaks can be recognized in all cases. To compare the simulation models, the k- ϵ model significantly differs ($\Delta H_t = 48\%$) from the laboratory results than the curves provided by the laminar model ($\Delta H_t = 33\%$) regardless of the outlet position. After 30 min experiment time, the model results approach the laboratory results at 26 mm outlet position. The difference between the model results is not significant. Moreover, the type of model does not have a remarkable effect on results. On the contrary, measurement with 7 mm outlet position the simulation results differ from laboratory results over a longer time.

Compare Fig. 6 with Fig. 5 (a), there is a linear tendency for laboratory measurement in Fig. 5 (a), while the CFD curves have an exponential shape. That is why peaks appear in Fig. 6 from 30 min to 90 min. The difference in results among CFD models and laboratory results can be caused because the CFD model was created to the end of the measurement, to the steady-state values. The aim was to approximate the time demand of homogenization measured in the outlet stream, instead of modeling the dynamics of the homogenization process, which is significant at the beginning of the experiment caused by the great density dissimilarity.

Afterwards, the ratio of homogeneity was calculated. The ratio is equal to the quotient of homogeneity of simulation and laboratory results at the same time. In Fig.7 (a) a peak is occurred in the first 20 min, later on, the values tend to 1 (red straight line), which means that the homogeneity is the same in case of the simulation and the laboratory measurement.

In order to observe the results articulately in the first 20 min, this part of the diagram is enlarged (Fig. 7 (b)). At both outlet position setups, the ratios of homogeneity are higher in case of the k- ϵ model than attained by laminar model. Observing the maximum ratio values at 7 mm outlet position, the homogeneity result obtained with the k- ϵ model is 34 times greater than in laboratory while this ratio was 19 in case of the laminar model. At 26 mm position setup the homogeneity is 45 times bigger with the k- ϵ model than in the laboratory. In the case of applying

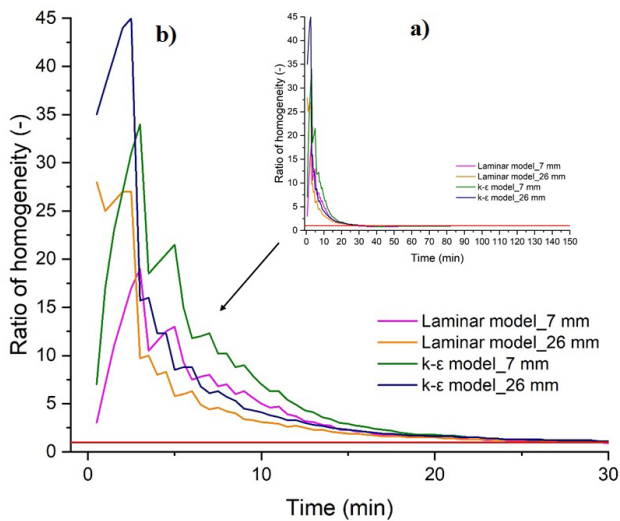


Fig. 7 The homogeneity ratio of different outlet positions and simulation methods compared to laboratory homogeneity a) over 150 min b) over the first 30 min

laminar model, this ratio is just 27. In conclusion, the figures indicate that laminar model is better to describe the concentration changes in the investigated tank.

In pursuance of analyzing the concentration change time by time, a plane between the outlet and the inlet was created in CFD models. In Fig. 8 concentration maps can be seen at different time, at the 26 mm outlet position setup. The density scale is between 1013.6 and 1002.2 kg m^{-3} in every time frame. Images show that the liquid is stirred layer by layer except of surrounding of the inlet. The inlet flow is penetrated into the liquid while the heavy layer is reached, then it is spread. Pictures indicate that the homogenization process was intensive in the first part of the measurements. In the last 100 min, concentration decline can be observed although it is not as sharp as before. The suction effect of the pump is not remarkable, however, some influence can be seen around the outlet. Furthermore, comparing the pictures at the same time but different CFD model, we can observe that the homogenization process is advanced applying k- ϵ model than with laminar model. In the case of the k- ϵ model, after 100 min mixing time density variation can not be recognized, in contrast with the laminar model where inhomogeneous fluid elements remained nearby the outlet.

In Fig. 9 inhomogeneity (%) (Eq. (14)) values calculated into the created plane can be seen in the function of notable sampling time (Fig. 8). Inhomogeneity was calculated with the help of the actual concentration difference ($c_t - c_{av}$) and the total concentration difference (Δc).

$$I_t (\%) = \left(\frac{|c_t - c_{av}|}{\Delta c} \right) \cdot 100 \quad (14)$$

In the case of 26 mm outlet position, the results affirm the observation before that the homogenization was occurring faster with the k- ϵ model than with the laminar model. Fig. 6 shows the same trend for 7 mm outlet position. Examine in contrast the results in point of outlet position, it can be assumed that homogenization in the constructed plane needs more time at 26 mm outlet than at 7 mm outlet position in case of the laminar model. In the aspect of using the k- ϵ model, significant differences cannot be recognized in results at varied outlet position.

3.3 Effect of outlet position

With the purpose to investigate in detail the influence of the outlet position from the perspective of homogenization, a 1 mm high outlet was created in CFD. This setup was referred to approximate the case when the outlet is absolutely at the bottom of the tank. Recirculation mixing was implemented with the same circumstances as in the previous examinations and stirring was accomplished with both models (Fig. 10).

According to use laminar model (Fig. 10 (a)) we can see that the outlet position affects the rate of homogeneity. In the case of 1 and 7 mm outlet position, at the beginning of the experiments, the homogeneity curves run together. The difference in the current homogeneity values was 2 % at varied outlet positions (1, 7 mm) in the same time. After 30 min, the curves start to move away from each other, and in the same time, 7 mm outlet position has higher ($H_t = 85\%$) homogeneity value than 1 mm setup ($H_t = 82\%$) has. The highest variance in homogeneity values (6 %) is appeared between 85 min to 95 min, notably, homogeneity is 99 % at 7 mm and 93 % at 1 mm setup. At 26 mm outlet position, the simulation result achieved by the laminar model (Fig. 10 (a)) is differed significantly from the results of other setups. In the same time, homogeneity values of 26 mm outlet position are higher than the others. From the aspect of the time demand to reach the 95 % homogeneity, remarkable difference is occurred. In case of 26 mm 65 min, at 7 mm 80 min and applying 1 mm outlet position 95 min is necessary to attain the given homogeneity value. Simulation with the k- ϵ model (Fig. 10 (b)) eventuates varied trend. In that case, the homogeneity results of 7 and 26 mm setup better approximate each other than 7 mm and 1 mm outlet position, especially at the beginning of the experiment. Homogeneity results carried out by k- ϵ model

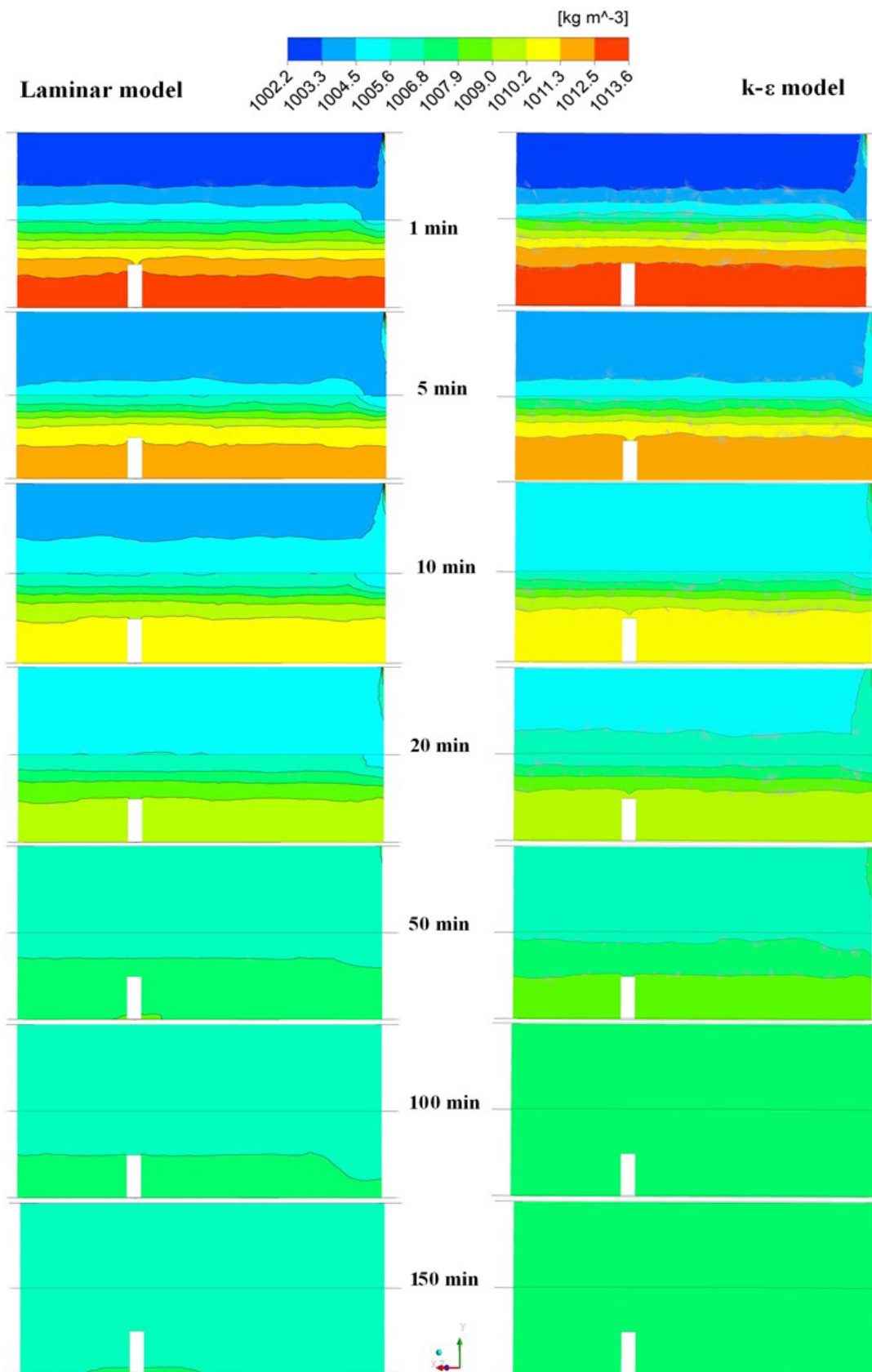


Fig. 8 Density maps in plane created between inlet and outlet at 26 mm outlet position setup

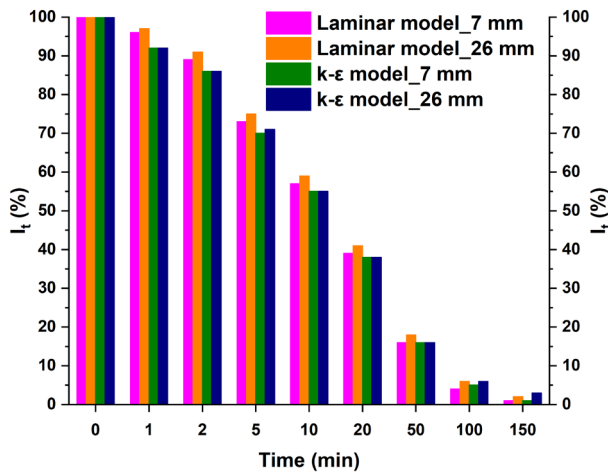


Fig. 9 Inhomogeneity results achieved by varied CFD models in the plane created between the inlet and the outlet at different sampling time

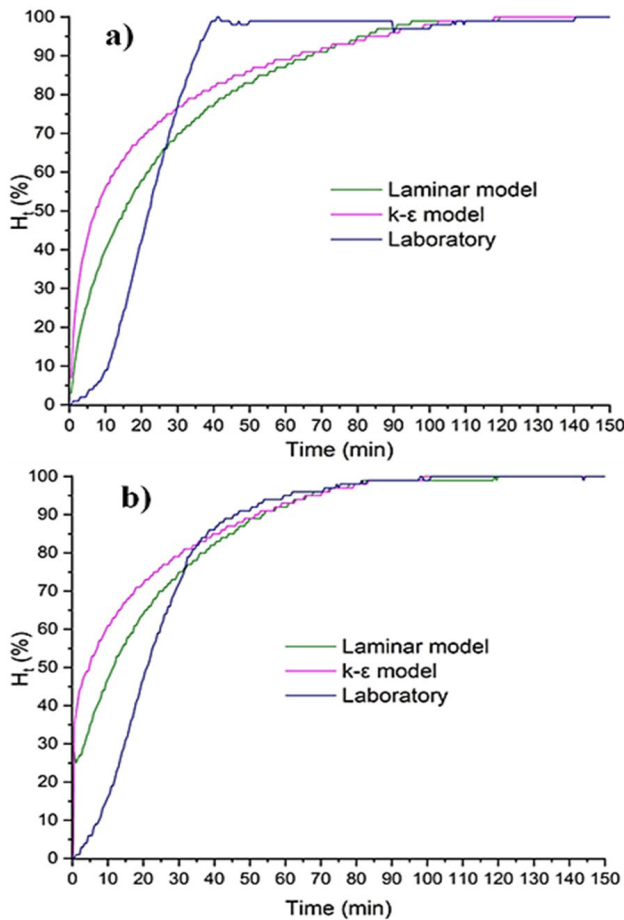


Fig. 10 Homogeneity at the outlet in case of different outlet height a) laminar model, b) k-ε model

at 26 mm are similarly higher as the laminar model than 1 and 7 mm positions own, as well as the rate with 7 mm, is over 1 mm homogeneity at the same time. To climb to the noted 95 % homogeneity rate, takes 65 min at 26 mm,

82 min at 7 mm and 88 min in case of 1 mm outlet position. Compare these time request with those, for which belong to the laminar model, and significant difference cannot be observed. Notable divergence can recognize at 26 mm outlet position, where 88 min takes with the k-ε model, and 95 min is required with the laminar model to reach 95 % homogeneity. The shortest time demand has the 26 mm setup in all cases that may be caused because this setup is the closest to the density line between the initial density layers.

In Fig. 11 we can see the difference in homogeneity in aspect of varied outlet positions between the k-ε model and the laminar model solution results. The curves show that the influence of the simulation method on results increases by the height of the outlet. At 26 mm and 7 mm outlet setup, the curves are maximized in a peak at the beginning of the experiments then these are begun to decline and stabilized around 0 %. That trend suggests that the applied model has influence on the dynamics of mixing instead of on the final rate of homogenization or on time demand of homogenization.

In Fig. 12 density maps of all outlet position setups can be seen in the plane which was created between inlet and outlet in case of the laminar model. The laminar model is chosen because the CFD results of the laminar model approach more appropriate the laboratory results (Fig. 7). In the first 20 min of the mixing process, remarkable difference cannot be recognized among the setups. The initial two-layer system is begun to break-up and new layers with dissimilar concentration have appeared. After 20 min, divergence can be observed among the setups principally between the 26 mm and the lower positions (7, 1 mm). The higher density solution is spread more effectively in the

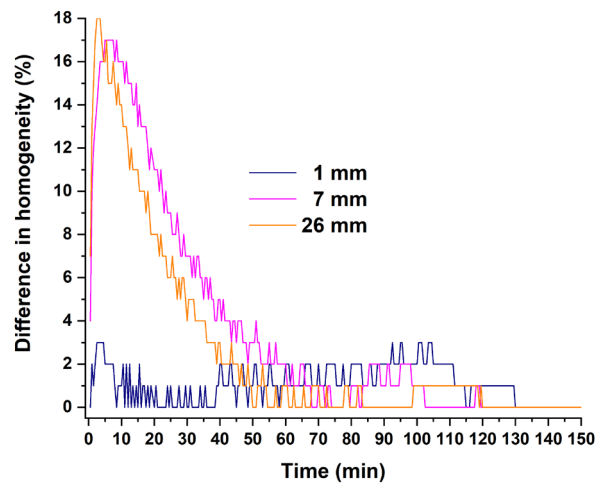


Fig. 11 The difference in homogeneity of the outlet results between the k-ε and the laminar model solution

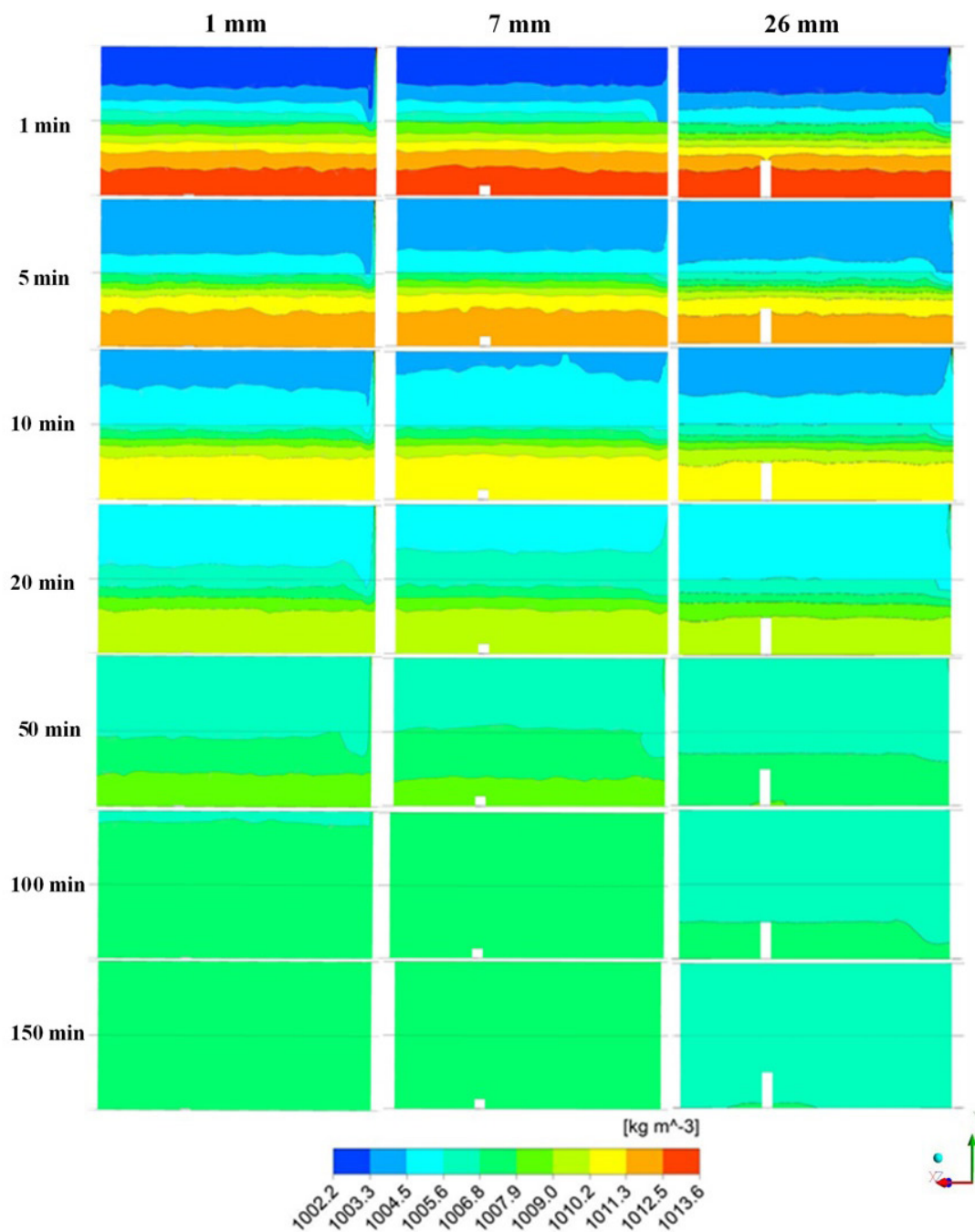


Fig. 12 Density maps in plane created between inlet and outlet at different outlet position setups in case of laminar model

upper part of the tank in case of lower positions than at 26 mm. Higher homogeneity degree is reached in case of lower setups at the same time. At the end of mixing, in case of 1 and 7 mm outlet positions homogeneous fluid body is realized in the created plane. Unlike at 26 mm outlet position where some inhomogeneous fluid elements remain nearby the outlet of the tank. In spite of the fact that the expected homogeneity is appeared earlier in the outlet stream at 26 mm setup (Fig. 10 (a)), the total fluid body may not absolutely homogenized.

4 Conclusion

In our study, a two-layer density stratified liquid was investigated in the aspects of homogenization. The mixing was achieved by external recirculation. The residence time was 3.53 h, which was chosen from an industrial example. Our aim was to research the mixing process in a system where stirring is carried out by external pump, as well as to examine the influence of the height of the outlet on homogenization. Two outlet setups were examined in the laboratory. The influence of the outlet position

was observed on homogenization at the outlet. After laboratory measurements had been finished, the content of the tank was mixed manually to convince that inhomogeneous fluid elements did not remain in the system. To investigate the mixing process in detail, the CFD model of the experimental tank was implemented in ANSYS Fluent. Two models were used namely, the laminar and the k- ϵ model. In case of both simulation methods, the results suggest that the mixing is achieved layer by layer. To compare the simulation results to laboratory results, one can state that the type of model has a remarkable impact on the dynamics of mixing instead of time demand of homogenization. The homogeneity results achieved by the k- ϵ model 45 times greater than at laboratory at the same time in the first 20 min of measurement. By contrast, at the laminar model, the homogeneity is just 27 times larger than the laboratory value. The results indicate that the laminar model describes more punctual the external mixing in the investigated tank. The influence of the position of the

outlet was appreciable in case of both models. The applied model type loses the significance of decreasing the outlet height. The time demand to get the expected concentration value at the outlet can be increased by the decrease of the outlet height; however, the results also imply that inhomogeneous fluid elements may remain in the tank. Consequently, to obtain the expected value in the outlet stream does not prove that the total fluid body is homogeneous. The density maps which were obtained by the laminar model imply that the lower height of the outlet improves to reach the homogeneous fluid body. It follows that 1 mm outlet position seems the most acceptable setup among the examined positions.

Acknowledgement

The authors of the paper would like to acknowledge the financial support of Széchenyi 2020 under the GINOP-2.2.1-15-2017-00059. We acknowledge the financial support of Széchenyi 2020 under the EFOP-3.6.1-16-2016-00015.

Nomenclature

| | |
|--------------------|--|
| c | concentration [kg m^{-3}] |
| c_t | concentration value in the current time [kg m^{-3}] |
| c_{av} | expected concentration value [kg m^{-3}] |
| Δc | difference between the initial and the expected concentration value [kg m^{-3}] |
| \mathbf{g} | gravitational acceleration $\mathbf{g} = \mathbf{g}(\mathbf{g}_x, \mathbf{g}_y, \mathbf{g}_z)$, [m s^{-2}] |
| k | turbulence kinetic energy [J kg^{-1}] |
| p | pressure [Pa] |
| \mathbf{v} | velocity vector $\mathbf{v} = \mathbf{v}(u, v, w)$ [m s^{-1}] |
| \mathbf{v}' | fluctuation velocity vector $\mathbf{v}' = \mathbf{v}'(u', v', w')$, [m s^{-1}] |
| $\bar{\mathbf{v}}$ | mean velocity vector $\bar{\mathbf{v}} = \bar{\mathbf{v}}(\bar{u}, \bar{v}, \bar{w})$ [m s^{-1}] |
| v_{av} | average velocity of falling film [m s^{-1}] |
| x, y, z | position in Cartesian coordinate system [mm] |
| A_0 | constant [kg m^{-3}] |
| A_1 | constant [-] |
| A_2 | constant [$\text{m}^3 \text{kg}^{-1}$] |
| B | volume rate of flow [$\text{m}^3 \text{s}^{-1}$] |
| $C_{1\epsilon}$ | model constant, $C_{1\epsilon} = 1.44$ [-] |
| C_2 | model constant, $C_2 = 1.9$ [-] |
| D | diffusion coefficient [$\text{m}^2 \text{s}^{-1}$] |
| D/Dt | substantial derivate [s^{-1}] |
| \mathbf{F} | force vector [N m^{-3}] |
| H_t | homogeneity (%) |

| | |
|--------------|--|
| ΔH_t | difference of homogeneity (%) |
| I_t | inhomogeneity (%) |
| L | fluid film thickness [m] |
| P_k | production of turbulence kinetic energy due to buoyancy force and mean velocity [$\text{J kg}^{-1} \text{s}^{-1}$] |
| W | cross section of the film [m^2] |

Greek symbols

| | |
|-------------------|--|
| δ | Kronecker unit vector $\delta_{ij} = 1$ if $i=j$, $\delta_{ij} = 0$ if $i \neq j$ |
| $\dot{\epsilon}$ | tensor of the deformation rate [-] |
| ϵ | rate of dissipation of turbulence kinetic energy [$\text{m}^2 \text{s}^{-3}$] |
| μ | dynamic viscosity [$\text{kg m}^{-1} \text{s}^{-1}$] |
| ν | kinematic viscosity [$\text{m}^2 \text{s}^{-1}$] |
| ν_T | kinematic eddy viscosity [$\text{m}^2 \text{s}^{-1}$] |
| ρ | density [kg m^{-3}] |
| σ_ϵ | TDR-Prandtl number, $\sigma_\epsilon = 1.2$ [-] |
| σ_k | TKE-Prandtl number, $\sigma_k = 1.0$ [-] |
| τ | shear stress tensor [$\text{kg m}^{-1} \text{s}^{-2}$] |
| φ | the angle between the plane and film [$^\circ$] |

Subscripts

| | |
|-----------|---|
| i, j, k | subscripts denoting Cartesian coordinate directions |
|-----------|---|

References

- [1] Blais, B., Lassaigne, M., Goniva, C., Fradette, L., Bertrand, F. "Development of an unresolved CFD-DEM model for the flow of viscous suspensions and its application to solid-liquid mixing", *Journal of Computational Physics*, 318, pp. 201–221, 2016.
<https://doi.org/10.1016/j.jcp.2016.05.008>
- [2] Ivleva, T. P., Merzhanov, A. G., Rumanov, E. N., Vaganova, N. I., Campbell, A. N., Hayhurst A. N. "When do chemical reactions promote mixing?", *Chemical Engineering Journal*, 168(1), pp. 1–14, 2011.
<https://doi.org/10.1016/j.cej.2011.01.002>
- [3] Vorobev, A. "Dissolution dynamics of miscible liquid/liquid interfaces", *Current Opinion in Colloid & Interface Science*, 19(4), pp. 300–308, 2014.
<https://doi.org/10.1016/j.cocis.2014.02.004>
- [4] Naeeni, S. K., Pakzad, L. "Experimental and numerical investigation on mixing of dilute oil in water dispersions in a stirred tank", *Chemical Engineering Research and Design*, 147, pp. 493–509, 2019.
<https://doi.org/10.1016/j.cherd.2019.05.024>
- [5] Karadimou, D. P., Papadopoulos, P. A., Markatos, N. C. "Mathematical modelling and numerical simulation of two-phase gas-liquid flows in stirred-tank reactors", *Journal of King Saud University – Science*, 31(1), pp. 33–41, 2019.
<https://doi.org/10.1016/j.jksus.2017.05.015>
- [6] Wei, P., Mudde, R. F., Uijtewaal, W., Spanjers, H., van Lier, J. B., de Kreuk, M. "Characterising the two-phase flow and mixing performance in a gas-mixed anaerobic digester: Importance for scaled-up applications", *Water Research*, 149, pp. 86–97, 2019.
<https://doi.org/10.1016/j.watres.2018.10.077>
- [7] Bensabath, T., Monnier, H., Glaude, P. A. "Acetylene pyrolysis in a jet-stirred-reactor for low pressure gas carburizing process – Experiments, kinetic modeling and mixing intensity investigations by CFD simulation", *Chemical Engineering Science*, 195, pp. 810–819, 2019.
<https://doi.org/10.1016/j.ces.2018.10.028>
- [8] Degawa, T., Fukue, S., Uchiyama, T., Ishikawa, A., Motoyama, K. "Behavior of a Jet Issuing Diagonally Upward into Two-Layer Density-Stratified Fluid in a Cylindrical Tank", *Journal of Flow Control, Measurement & Visualization*, 5(3), pp. 51–64, 2017.
<https://doi.org/10.4236/jfcmv.2017.53004>
- [9] Farooq, A., Shafaghhat, H., Jae, J., Jung, S. C., Park, Y. K. "Enhanced stability of bio-oil and diesel fuel emulsion using Span 80 and Tween 60 emulsifiers", *Journal of Environmental Management*, 231, pp. 694–700, 2019.
<https://doi.org/10.1016/j.jenvman.2018.10.098>
- [10] Derksen, J. J. "Blending of miscible liquids with different densities starting from a stratified state", *Computers & Fluids*, 50(1), pp. 35–45, 2011.
<https://doi.org/10.1016/j.compfluid.2011.06.013>
- [11] Cortada-Garcia, M., Wheliye, W. H., Dore, V., Mazzei, L., Angeli, P. "Computational fluid dynamic studies of mixers for highly viscous shear thinning fluids and PIV validation", *Chemical Engineering Science*, 179, pp. 133–149, 2018.
<https://doi.org/10.1016/j.ces.2018.01.010>
- [12] Nauman, E. B., Armstrong, M., Horak, J. "Static mixers for laminar flow reactors with low aspect ratios", *Chemical Engineering and Processing: Process Intensification*, 49(7), pp. 649–652, 2010.
<https://doi.org/10.1016/j.cep.2009.06.005>
- [13] Liu, M. "Age distribution and the degree of mixing in continuous flow stirred tank reactors", *Chemical Engineering Science*, 69(1), pp. 382–393, 2012.
<https://doi.org/10.1016/j.ces.2011.10.062>
- [14] Liu, D., Tang, W., Wang, J., Xue, H., Wang, K. "Comparison of laminar model, RANS, LES and VLES for simulation of liquid sloshing", *Applied Ocean Research*, 59, pp. 638–649, 2016.
<https://doi.org/10.1016/j.apor.2016.07.012>
- [15] Rosseburg, A., Fitschen, J., Wutz, J., Wucherpfennig, T., Schlüter, M. "Hydrodynamic inhomogeneities in large scale stirred tanks – Influence on mixing time", *Chemical Engineering Science*, 188, pp. 208–220, 2018.
<https://doi.org/10.1016/j.ces.2018.05.008>
- [16] Ascanio, G. "Mixing time in stirred vessels: A review of experimental techniques", *Chinese Journal of Chemical Engineering*, 23(7), pp. 1065–1076, 2015.
<https://doi.org/10.1016/j.cjche.2014.10.022>
- [17] Ochieng, A., Onyango, M. S. "Homogenization energy in a stirred tank", *Chemical Engineering and Processing: Process Intensification*, 47(9-10), pp. 1853–1860, 2008.
<https://doi.org/10.1016/j.cep.2007.10.014>
- [18] Welty, J. R., Wicks, C. E., W., Robert E. W., Rorrer. G. L. "Fundamentals of Momentum, Heat, and Mass Transfer", John Wiley & Sons, Inc., Castleton, NY, USA, 2007.
- [19] Launder, B. E., Spalding. D. B. "The numerical computation of turbulent flows", *Computer Methods in Applied Mechanics and Engineering*, 3(2), pp. 269–289, 1974.
[https://doi.org/10.1016/0045-7825\(74\)90029-2](https://doi.org/10.1016/0045-7825(74)90029-2)